

Alma Mater Studiorum Università di Bologna
Archivio istituzionale della ricerca

Tribochemical Conversion of Methane to Graphene and Other Carbon Nanostructures: Implications for Friction and Wear

This is the final peer-reviewed author's accepted manuscript (postprint) of the following publication:

Published Version:

Ramirez G., Eryilmaz O.L., Fatti G., Righi M.C., Wen J., Erdemir A. (2020). Tribochemical Conversion of Methane to Graphene and Other Carbon Nanostructures: Implications for Friction and Wear. ACS APPLIED NANO MATERIALS, 3(8), 8060-8067 [10.1021/acsanm.0c01527].

Availability:

This version is available at: <https://hdl.handle.net/11585/780152> since: 2020-11-12

Published:

DOI: <http://doi.org/10.1021/acsanm.0c01527>

Terms of use:

Some rights reserved. The terms and conditions for the reuse of this version of the manuscript are specified in the publishing policy. For all terms of use and more information see the publisher's website.

This item was downloaded from IRIS Università di Bologna (<https://cris.unibo.it/>).
When citing, please refer to the published version.

(Article begins on next page)

This is the final peer-reviewed accepted manuscript of:

Giovanni Ramirez, Osman Levent Eryilmaz, Giulio Fatti, Maria Clelia Righi, Jianguo Wen, and Ali Erdemir, *Tribochemical Conversion of Methane to Graphene and Other Carbon Nanostructures: Implications for Friction and Wear*, ACS Applied Nano Materials 2020 3 (8), PP. 8060-8067.

The final published version is available online at:
<https://doi.org/10.1021/acsanm.0c01527>

Rights / License:

The terms and conditions for the reuse of this version of the manuscript are specified in the publishing policy. For all terms of use and more information see the publisher's website.

This item was downloaded from IRIS Università di Bologna (<https://cris.unibo.it/>)

When citing, please refer to the published version.

1 Tribochemical Conversion of Methane to Graphene and Other 2 Carbon Nanostructures: Implications for Friction and Wear

3 Giovanni Ramirez, Osman Eryilmaz, Giulio Fatti, Maria Clelia Righi, Jianguo Wen,* and Ali Erdemir*



Cite This: <https://dx.doi.org/10.1021/acsanm.0c01527>



Read Online

ACCESS |



Metrics & More



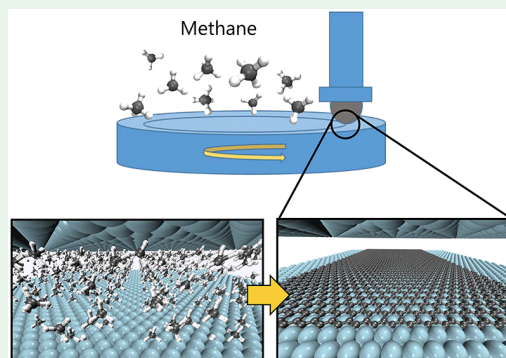
Article Recommendations



Supporting Information

4 **ABSTRACT:** Tribochemistry involves chemical reactions occurring at sliding
5 contact interfaces in the presence of gaseous and/or liquid media. It often leads
6 to the formation of a solid reaction film (also termed boundary film) which
7 controls friction and wear and hence the efficiency and reliability of moving
8 mechanical systems (such as engines). Here we demonstrate tribochemical
9 conversion of methane to graphene, nano-onion, and disordered carbons on
10 the sliding surfaces of Ni-, Cu-, and CuNi-containing VN coatings at
11 atmospheric pressure and room temperature, providing 2–3 orders of
12 magnitude reduction in wear and ~50% reduction in friction compared to
13 those of the uncoated steels. Transmission electron microscopy confirms that
14 graphene forms preferably on metal rich nanoclusters of the composite
15 coatings, while the carbon nano-onions are scattered throughout the carbon
16 tribofilm. Ab initio molecular dynamics simulations elucidate underlying
17 mechanisms involved in the tribochemical conversion of methane to carbon-
18 based nanostructures in support of microscopic observations. These scientific findings may lead to new materials technologies that
19 can use methane as a source for continuous and in situ lubrication. For example, there is an urgent need to curtail the uses of
20 lubricating oils in natural gas compressors and engines as they contaminate the natural gas being compressed or burnt.

21 **KEYWORDS:** tribochemistry, catalysis, carbon nanostructures, friction, wear, thin films/coatings



1. INTRODUCTION

22 Tribochemical reaction films (or tribofilms) are very typical of
23 all interacting surfaces that are in relative motion.¹ These films
24 commonly result from a chemical and/or catalytic response of
25 sliding surface to the reactive gases or liquids present at or in
26 the vicinity of sliding contact interface.² For example, the
27 formation of a phosphate glass-based tribofilm on rubbing
28 surfaces of engine components is extremely important for long
29 life or reliability and is a direct result of tribochemical reactions
30 occurring between sliding surfaces and zinc dialkyl-
31 dithiophosphate (ZDDP) antiwear additive in engine oils.³
32 Likewise, a dramatic reduction of friction (i.e., from ~0.6 to
33 ~0.003) in ta-C and CN_x type carbon coatings in hydrogen
34 environment is due to a tribochemical reaction between
35 surface carbon atoms and hydrogen, creating a fully hydrogen
36 terminated or passivated top surface layer that diminishes
37 adhesion and hence friction during sliding.⁴ Overall, the
38 making and breaking of such tribofilms dominate friction and
39 wear and hence the durability and frictional performance of all
40 moving mechanical systems.

41 Besides these liquid and gaseous species, all kinds of solid
42 lubricants are available^{5,6} for controlling friction and wear. In
43 addition to the traditional graphite, molybdenum disulfide, and
44 boron nitride,⁷ many researchers have confirmed that low-
45 dimensional nanomaterials like fullerenes,⁸ graphene,^{9,10} nano-

tubes,¹¹ and nano-onions, are also very effective in reducing
friction and wear.¹² One major drawback is that mainly
because of their finite thickness or volume, these solids tend to
wear out eventually, and thus high friction and wear prevail
again.

Here we report tribochemical conversion of methane (CH₄)
to graphene, nano-onion, and disordered carbons on the
sliding surfaces of Ni-, Cu-, and CuNi-containing VN coatings
under atmospheric pressure and at room temperature. We
show that these catalytically active coatings enable in-operando
extraction of graphene and other carbon nanostructures
continuously from CH₄, thus providing extraordinary protec-
tion against wear and lowering friction. Obviously there are not
many moving mechanical assemblies that operate in CH₄, but
it is a major constituent of natural gas for power generation
and fueling of transportation systems in which many moving
parts operate in natural gas, including pistons and seal packs of
reciprocating natural gas compressors in pipelines, refueling

Received: June 3, 2020

Accepted: July 16, 2020

Published: July 16, 2020

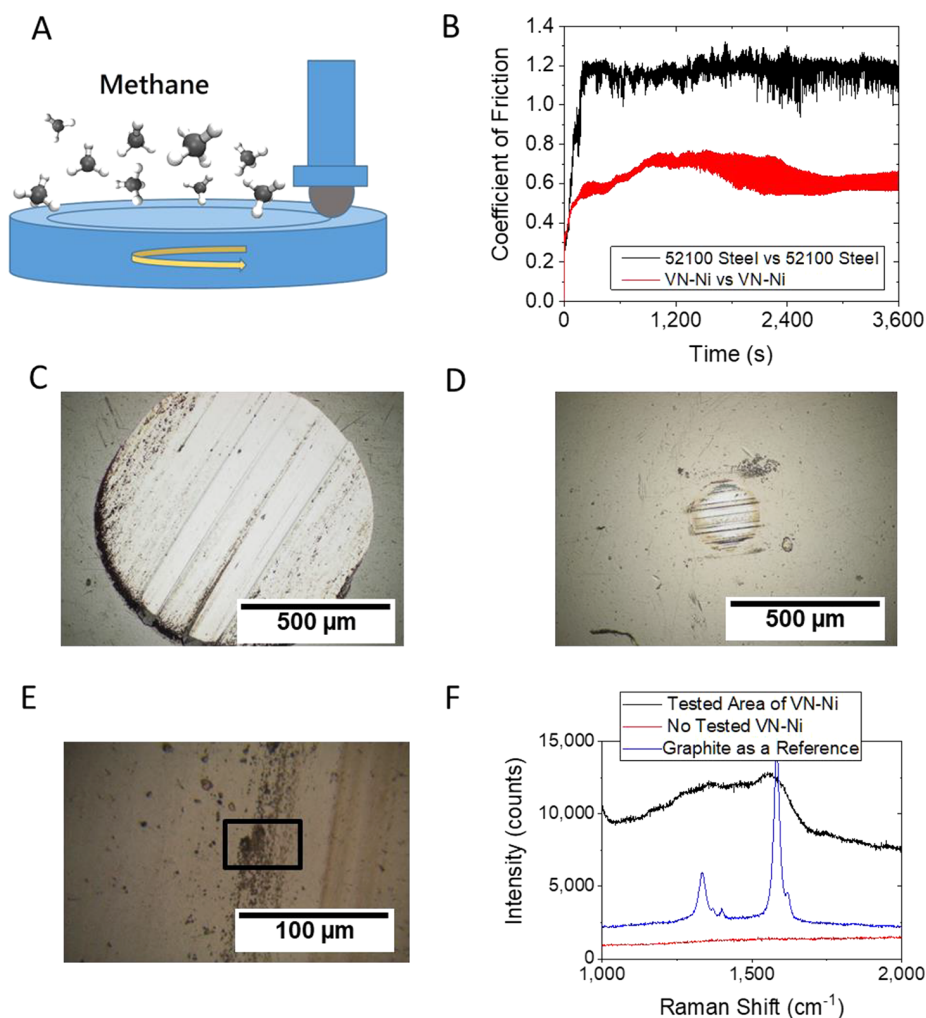


Figure 1. Comparison of friction and wear behaviors in ball-on-flat tests. (A) Schematic illustration of test method and environment. (B) Friction coefficient of uncoated AISI 52100 steel sliding against the same material compared with that of VN-Ni-coated AISI 52100 steel sliding against the same material in 960 bar of CH₄ gas. (C) Size of wear scar formed on uncoated AISI 52100 steel ball in CH₄. (D) Size of wear scar formed on VN-Ni-coated AISI 52100 steel ball in CH₄. (E) SEM image of wear track on VN-Ni-coated surface with blackish wear debris layer. (F) Raman spectra obtained from the area denoted with a black rectangle showing broad D and G bands located in the same position as the ones corresponding to the graphite used as a reference.

stations, and the fuel injectors of natural gas-powered engines.¹³ Therefore, the results of our study are not only scientifically significant but also have the capacity of positively influencing these fields by leading to more efficient, durable, and cost-effective industrial practices. In particular, enabling hydrocarbon molecules of natural gas to provide a composite carbon tribolayer on a self-replenishing or self-healing manner is very attractive.

2. RESULTS

2.1. Friction and Wear Performance. Details of the coating deposition procedure, structural, chemical, and mechanical characterization of resultant coatings as well as the tribological test methodology and conditions are provided in the [Supporting Information](#) (see Figures S1–S3). Under the test configuration illustrated in [Figure 1a](#), the friction coefficient of a steel ball sliding against the steel flat in CH₄ goes up very quickly to a value of 1.2 and remains relatively constant until the end of the 2 h long test ([Figure 1b](#)). When the same test was repeated with a VN-Ni-coated test pair, the friction coefficient was reduced by nearly 50%. More

remarkably, the wear volume loss on the coated ball side was reduced by more than 2 orders of magnitude (i.e., 245 times; see [Figures 1c,d](#)), going from $7.7 \times 10^{-12} \text{ m}^3$ when steel vs steel surfaces were tested ([Figure 1c](#)) down to $3.14 \times 10^{-14} \text{ m}^3$ for the VN-Ni vs VN-Ni test case ([Figure 1d](#)). The wear damage on the uncoated 52100 steel flat was also very extensive, as a very wide and deep wear groove had formed, while on the VN-Ni-coated flat side, the wear damage was hard to discern ([Figure 1e](#)). Additional supporting results (obtained from two other coatings: VN-CuNi and VN-Cu) further confirmed the unusual wear reducing abilities of these composite coatings in the presence of CH₄ ([Figure S4](#)).

2.2. Characterization of Sliding Surfaces. Upon close examination of the sliding surfaces of VN-Ni-coated test pairs with a microscope, we noticed some blackish wear particles or patches at or near the rubbing surfaces of both the ball and flat surfaces, as highlighted with the rectangles in [Figures 1d,e](#). Also, in [Figure 1f](#), the Raman spectra of these black deposits display a signature that overlaps with the D and G bands of crystalline graphite (which was used as a reference). These results suggest that the blackish debris that

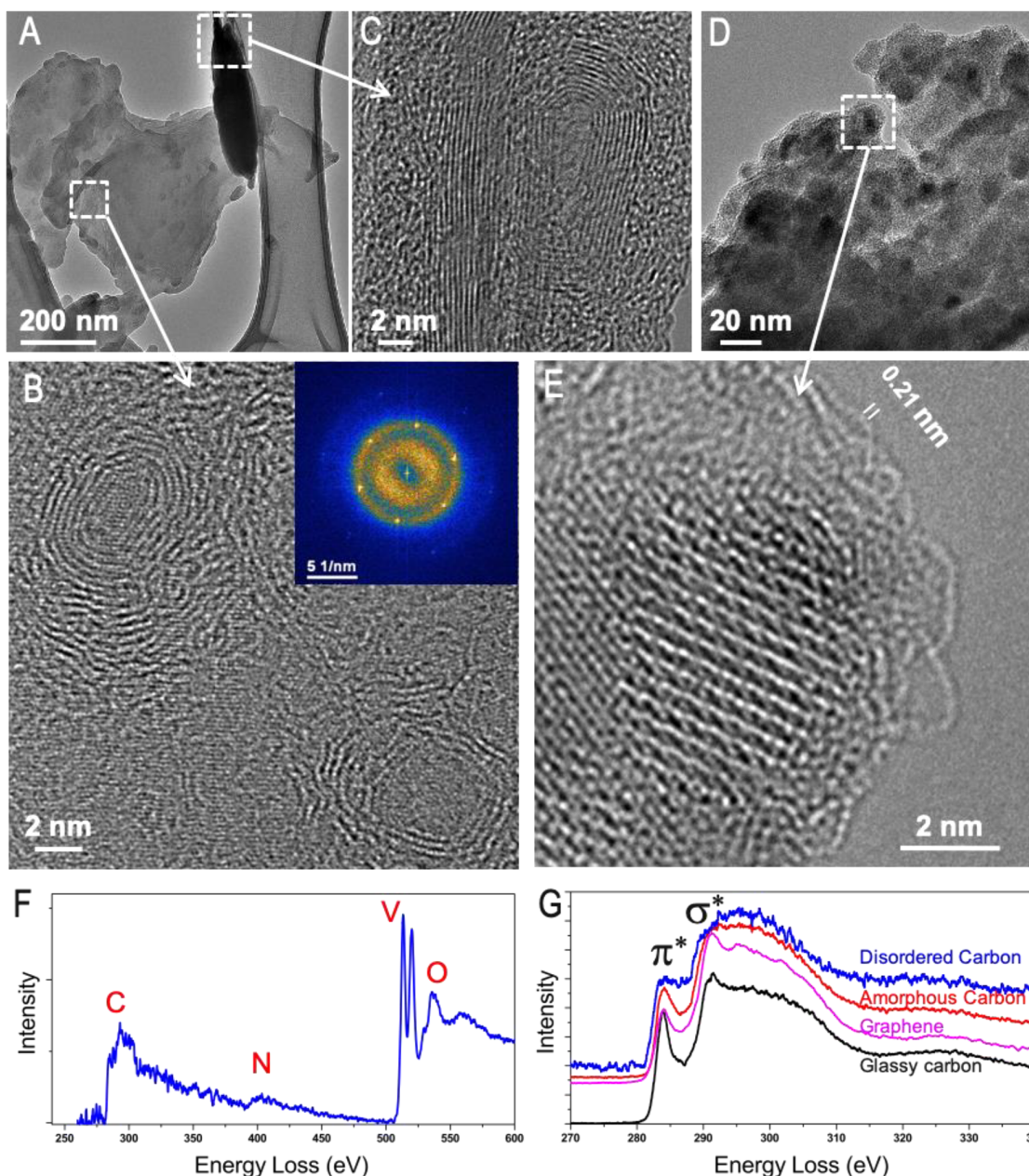


Figure 2. TEM study of debris particles. (A) Low-magnification and (B) HRTEM images of large graphene sheet with scattered carbon nano-onions. (C) TEM image showing side view of carbon nano-onions attached on a graphene sheet (about 10 layers). (D) Low-magnification and (E) HRTEM images of agglomerated nanoparticles wrapped with highly disordered carbon. (F) EELS spectrum from agglomerated debris showing almost no N. (G) EELS spectra of carbon K-edge of disordered carbon compared with glassy carbon (standard), graphene (from image B), and amorphous carbon on the TEM grid.

was detected on and around the rubbing surfaces of the coated ball and flat samples had a structural chemistry that is analogous to that of the reference material graphite. Overall, the results in Figure 1 clearly show that the VN-Ni coating provided much lower wear in CH₄, and this improvement was most likely due to the formation of a carbon-rich tribofilm derived from the CH₄ gas during sliding experiment (Figure 1a). Results from VN-CuNi and VN-Cu (presented in Figure S4) were similar and in support of the findings shown in Figure 1. Specifically, remarkable improvements in their friction and wear performance were also associated with the formation of a blackish tribofilm on or near their rubbing surfaces.

We recovered a portion of the debris particles from the area highlighted with the rectangle in Figure 1e using a metallic tip and placed it onto a copper grid for transmission electron microscopy (TEM). The TEM images in Figure 2 show two major types of debris: graphene with carbon nano-onions (Figures 2a–c) and an agglomeration of numerous nanoparticles wrapped by highly disordered graphitic carbon (Figures 2d,e). The first type is mainly a large graphene sheet ranging from 500 nm to several micrometers in size, as shown in Figure 2a. High-resolution transmission electron microscopy (HRTEM) showed that the graphene sheets are composed of a single layer (Figure 2b) to about 10 layers (Figure 2c). Single-layer graphene was confirmed by an

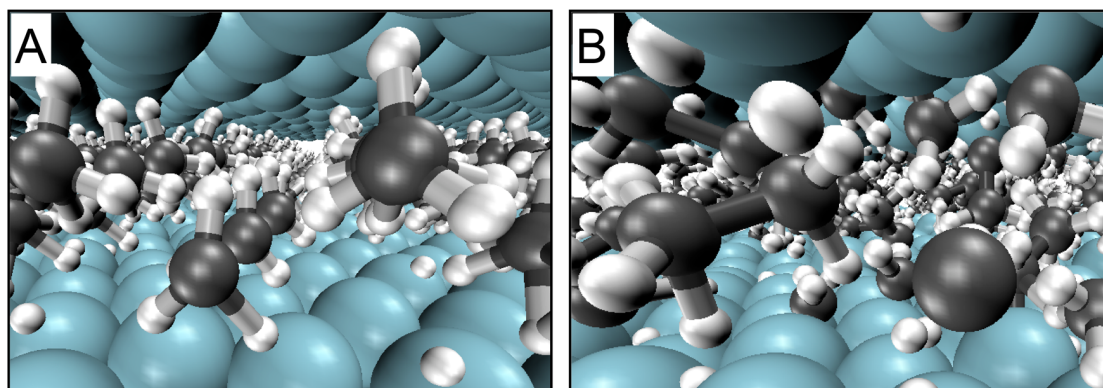


Figure 3. AIMD simulation of methane molecules confined at Ni interface during sliding. (A) Initial system configuration with undissociated methane molecule. (B) Snapshot acquired after ~ 2 ps of AIMD at constant load and shear velocity: the molecules started dissociating and H atoms diffusing below the surfaces. The full simulation movie ([Movie S1](#)) is available as [Supporting Information](#).

HRTEM image at broken edges (see [Figure S5](#)). Carbon nano-onions with diameters of 5–10 nm were scattered on the graphene sheet, as highlighted in [Figures 2b,c](#), throughout the examined area. These carbon nano-onions are hollow in the center, and no other crystalline form of carbon structure is observed. Compositional analyses by energy-dispersive X-ray spectroscopy (EDS) and electron energy-loss spectroscopy (EELS) showed that the nano-onions are composed of graphene with a small amount of Ni and V (see [Figure S5](#)). The small amounts of Ni and V could act as catalysts for the growth of graphene and carbon nano-onions.

3. DISCUSSION

Results presented above demonstrate that the VN-Ni coating can convert CH_4 into graphene, carbon nano-onion, and disordered carbon, all of which are known for their favorable antifriction and antiwear properties.^{8,9,12} Specifically, friction was reduced by 50%, and the wear was reduced by a factor of 245 (other systems tested, i.e., VN-CuNi and VN-Cu, have also exhibited remarkable reductions in wear (as much as 3 orders of magnitude) as presented in [Figure S4](#)). As is evident from [Figure 1b](#), the reduction in friction is not as dramatic as in wear. This is mainly due to the incomplete coverage of sliding surfaces with a continuous layer of graphene and other carbon forms. Specifically, because of their very soft nature, they are prevented from thickening into a continuous tribofilm under the influence of high contact pressure and shear forces exerted on them. Instead, they are ejected from the interface and accumulated around the edges of the wear scar and track as highlighted with rectangles in [Figures 1d,e](#). In addition, the shear properties of graphene and other carbon nanostructures are not as favorable in nitrogen and methane.

We believe that the Ni, Cu, and CuNi are most likely acting as catalysts for the tribochemical conversion of CH_4 into graphene, nano-onion, and disordered carbon (since such carbon structures were only found in and around the sliding contact areas). Ni and Cu are used extensively in the synthesis of graphene, nanotubes, and nano-onions by chemical vapor deposition (CVD) at high temperatures.¹⁴ The specific steps involved in the catalytic conversion of hydrocarbon gases into graphene by CVD method using Ni, Cu, and other transition metals are well-documented.^{15–18} Briefly, these studies have suggested that partially filled d-orbitals of Ni (or Cu) enable them to adsorb hydrocarbon molecules first and then facilitate their dehydrogenation. Liberated carbon atoms are free to

migrate throughout the surface (as well as bulk) and eventually come together to form the planar sheets of carbon as in graphene.¹⁴ Also, vanadium nitride probably contributed to the catalytic dehydrogenation of CH_4 to some extent, despite its catalytic activity being much lower than that of transition metals,^{19–21} as is confirmed by means of ab initio calculations in [section 3.1](#). However, VN presents high resistance to thermal degradations because of its high thermal stability and thus helps prevent film fracture and due to thermal stresses.²²

In our case, there was no similarity to the traditional CVD synthesis route, rather a situation involving two VN-Ni (or VN-Cu, VN-CuNi)-coated solid surfaces pressed against one another in relative motion in the presence of CH_4 at ambient pressure and temperature. Yet, these rubbing surfaces were able to extract graphene and other carbon nanostructures in a continuous manner from the methane gas and thereby enable ultrahigh resistance against wear. In an attempt to understand the molecular-level mechanisms of tribochemical conversion of CH_4 to mentioned carbon nanostructures at sliding contact interfaces, we concentrated on VN-Ni-coated test pairs and conducted *ab initio* molecular dynamic simulation on them as discussed below.

Because of the very complex nature of the physical, chemical, and tribological events taking place at a sliding contact interfaces, understanding the exact mechanisms by which graphene, carbon nano-onion, and disordered graphitic carbons are derived from CH_4 on VN-Ni and other surfaces (i.e., VN-Cu and VN-CuNi) will be rather challenging. In particular, determining time and spatial resolutions of events leading to the formation of such carbonaceous nanostructures is deemed impossible with currently available tribological methods. However, it is conceivable that under the tribological contact configuration shown in [Figure 1a](#) and conditions described in the [Supporting Information](#) (i.e., a high-pressure mechanical shearing action combined with transient high flash heating of real contact spots²³) the tribochemical extraction of such carbon nanostructures from CH_4 may become feasible. Specifically, the high-pressure rubbing action continuously creates nascent surface atoms^{24–26} of the catalyst metals (Ni, Cu, and NiCu) which enhance catalytic and hence the tribochemical activity toward methane in the surrounding environment. As mentioned above, both Ni and V are well-known catalysts used previously in the synthesis of graphene and carbon nanotubes by high-temperature CVD methods.^{15–18} Their lower activation energy for dissociative

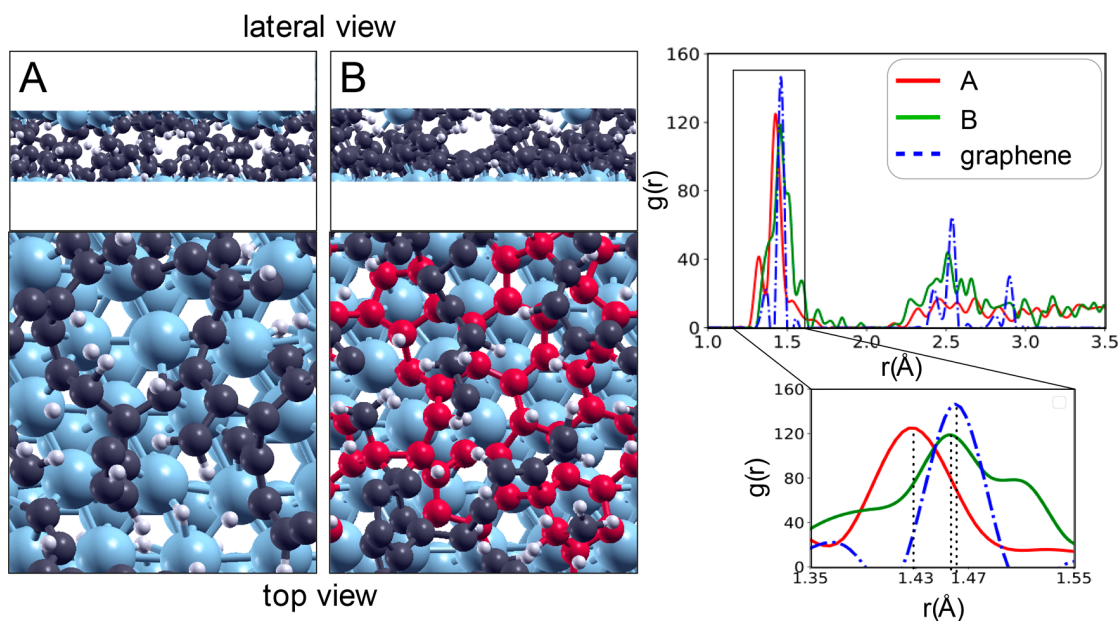


Figure 4. First stages of tribologically induced graphene formation. Snapshots acquired during AIMD simulations of dehydrogenated methane molecules confined at Ni interfaces in concentrations corresponding to 50% (A) and 100% (B) coverages of the Ni interface. (A) In a first stage the C atoms bind to each other in interconnected chains that form a disordered, low-density film. (B) Load and shear stresses applied promote the rehybridization of C atoms and the formation of sp^2 planar structures as the graphene flake highlighted in green. (C) The corresponding radial distribution functions for C–C bonds are represented by red and green lines, respectively, while the dashed-dot blue line indicates the radial distribution function of a nondefective graphene layer commensurate with the Ni (111) surface. The full simulation movies (Movies S2 and S3) are available as [Supporting Information](#).

217 extraction of carbon from methane and hence facilitate the
218 formation of such carbon materials. In the following section,
219 we present the results from *ab initio* molecular dynamics
220 (AIMD) simulations to provide further insight into the
221 atomistic mechanisms that govern the tribochemically induced
222 formation of carbon nanostructures.

223 3.1. Tribochemical Mechanism by Means of *Ab Initio*

224 **Calculations.** First, we evaluated the catalytic capability of the
225 Ni and VN substrates in promoting the CH_4 dehydrogenation
226 by means of *ab initio* static calculations. The results of this
227 study, which are reported as [Supporting Information](#) (Figures
228 S10–S12), are in agreement with the literature in the case of
229 Ni,^{27–30} while we are not aware of any previous study for VN.
230 The reaction energies calculated for methane dissociation on
231 Ni (111) and VN (100) surfaces, which are the most stable
232 surfaces for these materials, correspond to 0.02 and 0.89 eV,
233 respectively. Therefore, at ordinary conditions, the full
234 dehydrogenation reaction, $CH_4 = C_{ads} + 4H_{ads}$, is not
235 energetically favorable. However, the molecular confinement,
236 mechanical stresses applied, and high temperatures present at
237 the tribological interface can promote the dehydrogenation
238 reaction at a very high rate, as shown by the *ab initio* molecular
239 dynamic (AIMD) simulation of CH_4 molecules confined at
240 sliding Ni interfaces, as described in the following.

241 In the AIMD simulations, both the electronic and the ionic
242 degrees of freedom were considered. This approach is essential
243 to obtain an accurate description of the chemical processes
244 occurring under conditions of enhanced reactivity. The first set
245 of simulations aimed at identifying the mechanisms of carbon
246 release from CH_4 molecules, while subsequent simulations,
247 where the concentration of interfacial carbon was increased,
248 were aimed at monitoring in real time the formation of carbon
249 nanostructures assisted by mechanical stresses.

The initial system configuration, shown in [Figure 3A](#),
contained a concentration of CH_4 molecules such that the
number of C atoms corresponded to 25% of the Ni interfacial
atoms. A normal pressure of 5 GPa was applied, and the upper
surface was moved at constant velocity of 200 m/s along the
[112] direction. The temperature of the Ni surfaces was kept
constant at 1000 K, while the intercalated molecules were left
free to evolve without any temperature control. The high
temperature is chosen to model the flash temperatures that,
depending on the ratio between the real contact area and the
apparent contact area, can rise up to thousands of kelvin.^{31,32}
However, the comparison with AIMD simulations performed
at 300 K, while leaving unchanged the other setup parameters,
which are presented in the [Supporting Information](#) (Figure
S12), shows that the temperature plays a secondary role in the
dehydrogenation process, which is to be attributed mainly to
molecular confinement under load and shear stresses.

As can be seen from the atom trajectories ([Movie S1](#)), the
dehydrogenation process started immediately after the
beginning of the dynamic simulation: H atoms detach from
 CH_4 molecules as soon as they come into contact with the
clean Ni surfaces. This result indicates that molecular
dissociation, which is energetically unfavorable at the open
surface, can be easily promoted at the tribological interface.
The molecular confinement under load and shear dramatically
reduces the activation time for molecular dissociation, as
previously found for water molecules confined at diamond
interfaces^{33–35} and organophosphorus additives at iron
interfaces.³⁶

The simulation then indicated H diffusion into the Ni bulk,
which leads to an increase of carbon concentration at the
interface. This is consistent with the above-described
experimental observation of newly formed carbon nanostruc-
tures almost H free. After ~ 2 ps, around 20% of the H atoms

had been expelled from the interface and diffused into the bulk. At the same time, more than half of the carbon atoms were adsorbed on the surfaces, where they tend to capture other C atoms, forming small hydrocarbon groups, C_nH_x with $n \leq 3$ (Figure 3B).

After ~ 3 ps from the beginning of the simulation, the interfacial concentration of H atoms decreased by more than 50% with respect to the initial value, and all the C atoms present at the interface become bonded either to surface Ni atoms or to other C atoms in short carbon chains, C_n with $n \geq 2$. Reactive carbon intermediates, C_n , have been also identified during the thermal decomposition of CH_4 on Ni(111) by the in-operando technique of near-ambient-pressure X-ray photoelectron spectroscopy.³⁷ Not observed were Ni_2C reconstruction and other carbide structures, which are often found during graphene growth on Ni (111). The origin of some differences with the structures observed during graphene growth may be related to the presence of a countersurface: the coordination of molecular fragments during the decomposition process is always higher at the interface than at the open surface, and this may for example limit the subsurface diffusion of carbon.

Figure 4 shows two snapshots acquired during AIMD simulations containing increased concentrations of C atoms, corresponding to 50% (A) and 100% (B) coverages of the Ni interface. The full adatom trajectories are presented in Movie S2 and Movie S3. In a first stage, we observed the formation of carbon chains, the length of which increased during the simulation until every interfacial C atom had been included into a chain branch (Figure 4A). The chains became cross-linked, forming a disordered film of low density. The applied load and shear smeared out this film, reducing more and more its thickness. During this rubbing process, the carbon atoms change their hybridization and start to form planar rings that constitute the first seeds for graphene growth. Indeed, we observed the formation of a graphene flake upon further increase of C coverage (Figure 4B). The shift of the peak of the C–C radial distribution functions from ~ 1.43 to ~ 1.47 Å (Figure 4C) clearly indicates the rehybridization from sp to sp^2 that accompanies the structural change from interconnected carbon chains to 2D structures. The similarity of the $g(r)$ function calculated for the structure in Figure 4B (green continuum line), which also presents a second peak, and the $g(r)$ calculated for a nondefective graphene layer commensurate to the Ni(111) surface (blue dashed-dotted line) provides a further evidence that graphene is being formed during the simulation under the tribological conditions.

Recently, it was shown that carbon-based tribofilms can also be derived from a variety of carbon-based liquids including synovial fluids that lubricate joints, poly(α -olefin) (PAO) which is a base oil used in the making of synthetic lubricants, and palm methyl ester (PME) which is a biodiesel fuel extracted from palm oil. Specifically, it was reported that a graphitic tribofilm forms on the rubbing surfaces of metal-on-metal (MOM) hip replacements (which are made of cobalt, chrome, and molybdenum),³⁸ MoN-Cu coatings³⁹ lubricated by a PAO oil, and AISI 304 stainless steel lubricated by PME.⁴⁰ MOM is suspected to derive graphitic tribofilm from protein molecules through the catalytic effects of Co and Mo, while in the cases of MoN-Cu and AISI 304 stainless steel, Cu and Ni present in their structures, respectively, are believed to help in the extraction of carbon-rich tribofilms from the PAO and PME molecules.

4. CONCLUSIONS

Our test results demonstrate that tribochemistry can play a major role in the friction and wear behavior of sliding surfaces. Specifically, under the high-pressure shearing condition described in our study, VN-Ni, VN-Cu, and VN-CuNi coatings can convert CH_4 molecules into graphene, nano-onion, and disordered graphite, which in turn reduce friction (by as much as 50%) and wear by 2–3 orders of magnitude (see Figure 1 and Figure S4). High catalytic reactivity of Ni and Cu in the composite coatings promotes tribochemistry and hence conversion of CH_4 to a carbon-based tribofilm consisting of graphene, nano-onion, and disordered carbons. Transmission electron microscopy (Figure 2) showed that graphene is preferably formed on and around the VN-Ni clusters, while nano-onions and highly disordered graphite were scattered throughout the carbon tribofilm. *Ab initio* MD simulations (Figures 3 and 4, Figures S10–S12, and Movies S1–S3) revealed the mechanism by which carbon nanostructures are extracted from CH_4 molecules. These simulations showed that the conversion of CH_4 to 2D graphene and nano-onions occurs by a catalytic process involving first the dehydrogenation of CH_4 on Ni followed up by C atoms forming chains of an amorphous carbon network of low atomic density. Under the influence of high contact pressure and shear forces, some of the amorphous carbon network sandwiched between the Ni surfaces undergoes rehybridization and subsequent conversion to sp^2 planar structures. These newly formed sp^2 -bonded hexagonal rings nucleate the first graphene flakes. Once such graphene-rich tribofilms are formed on sliding surface, wear is reduced dramatically (as much as 3 orders of magnitude).^{40–42} Overall, our study demonstrates the critical role of tribochemistry in the extraction of low-shear and highly protective carbon tribofilms from CH_4 and hence the reduction of friction and wear. Such carbon-based protective tribofilms could be utilized and produced on demand in natural gas compressors and engines, eliminating the use of oils that contaminate natural gas and diminish the need for frequent oil change continuous resupply.

5. MATERIALS AND METHODS

Test materials used in this study included coated steel balls rubbing against coated flats made from AISI 52100-grade through-hardened ball bearing steel (nominal hardness, 58–62 Rockwell C). Prior to the deposition of Ni-, Cu-, and CuNi-containing VN coatings, Ar sputter ion etching is conducted to remove the surface contaminants. Subsequently, a V bonding layer (120 nm thick) was deposited first on the steel substrate by using a dual magnetron sputtering system. The nanocomposite coatings were deposited from high-purity targets (i.e., V (99.95%) and Cu, Ni (99.99%). For example, to prepare the VN-Ni nanocomposite coatings (containing ~ 9.5 at. % of nickel), 4000 W (9 W/cm^2) and 225 W (5.1 W/cm^2) were applied on V and Ni targets, respectively. The substrate temperature was kept constant at 325°C . The total working pressure was fixed at 0.4 Pa in a mixture of Ar/ N_2 (120 sccm/80 sccm, respectively).

As the next step, a crystallographic phase analysis was performed of the composite coatings (about $1 \mu\text{m}$ thick) by using an X-ray diffractometer (Bruker D2 Phaser) with the monochromatized Cu $K\alpha$ radiation. The hardness and elastic modulus of the coatings were measured by a nanoindenter (Hysitron Triboindenter TI-950) with a Berkovich diamond probe. Different loads (0.5–12 mN) were used to evaluate the hardness/elastic modulus as a function of the penetration (h_c) to avoid the influence of the substrate mechanical properties. The Oliver–Pharr⁴³ method was used to calculate the hardness and the elastic modulus of the coatings. The surface roughness of the as-

received and coated surfaces was measured by a Bruker Contour GT white light 3D profilometer.

Sliding experiments were performed with a high-vacuum tribometer using a ball-on-disk setup, in which a stationary steel ball (9.5 mm in diameter) was pressed against a rotating disc (50.8 mm and 6.35 mm thick) under mean Hertz pressures of ~ 0.6 GPa. Both coated and uncoated balls were tested against the coated/uncoated steel flats in the presence of atmospheric pressure methane at room temperature. The sliding contact surfaces of ball and flat specimens had a nominal surface roughness of $0.02\ \mu\text{m}$ RMS. Prior to the tribological tests, all test samples were cleaned by acetone and isopropanol solvents in an ultrasonic bath for 5 min. The pure methane gas was bled into the vacuum chamber after evacuating it down to 10^{-4} Pa levels until reaching 0.9 atm (~ 91 MPa). The experiment was performed at room temperature. The normal load on top of the stationary ball was 2 N (which would create a peak Hertz pressure of ~ 0.6 GPa), and the sliding speed was 0.1 m/s, so that the rubbing surfaces would have been under severe contact conditions at all times. The total sliding distance accumulated during the tests was 360 m. The friction force generated between the sliding ball and flat surfaces was continuously monitored and recorded throughout the tests using a data acquisition system and later converted to the friction coefficients for the entire test cycle.

The wear volumes on the ball and disk samples were assessed with the help of optical microscopy; specifically, the wear scars and tracks were imaged by an Olympus STM6 microscope. The amount of wear was calculated by using the standard wear volume equations based on the wear scar diameter measured by the microscope.

The tribofilms were analyzed by confocal Raman microscopy (inVia Reflex, Renishaw, Inc.) using appropriate light sources with a wavelength of 633 nm to determine the nature of the tribochemical films that formed on the rubbing surfaces during sliding. The Raman instrument was calibrated with an internal silicon reference, and the spectra were recorded in the range $1000\text{--}2000\ \text{cm}^{-1}$. Highly oriented pyrolytic graphite (Ted Pella, lacey carbon) was used as a reference.

Density functional theory calculations were performed within the generalized gradient approximation in the Perdew–Burke–Ernzerhof parametrization.⁴⁴ The ionic species were described by ultrasoft pseudopotentials, and the electronic wave functions expanded in plane waves.⁴⁵ A kinetic energy cutoff of 25 Ry (200 Ry) was used to truncate the expansion of the wave functions (charge density) on the basis of test calculations on the bulk properties of the considered materials. The static calculations were performed by means of periodic supercells containing a vacuum region 15 Å thick and a slab with (2×2) in-plane size and three layers thickness. The in-plane size of the cell was increased to a $4 \times 3 \sqrt{3}$ cell, corresponding to 24 atoms per layer, in dynamic calculations. Although nickel is known to be ferromagnetic, we did not consider the spin polarization to avoid a dramatic increase of the computational workload of the *ab initio* molecular dynamics simulations, where the reaction paths are mainly governed by the mechanical stresses applied. This computational choice is also justified by previous works on C/CH_x chemisorption and CH₄ dehydrogenation on Ni.^{27,28,30}

Ab initio molecular dynamics simulations were performed in the Born–Oppenheimer scheme using a home-modified version of the program included in the Quantum Espresso package that permits the user to simulate tribological conditions. In particular, a constant load and a constant relative velocity of the two surfaces have been modeled. We controlled the temperature of the two sliding slabs (excluding the translational motion), while leaving the temperature of the intercalated molecules free to evolve.

■ ASSOCIATED CONTENT

SI Supporting Information

The Supporting Information is available free of charge at <https://pubs.acs.org/doi/10.1021/acsanm.0c01527>.

Coating characterization (Figures S1–S3); tribological characterization (Figure S4); tribofilm characterization (Figures S5–S9); computational results (Figures S10–

S12); captions for Movies S1–S3; supplementary References (1–9) (PDF)

Movie S1 (MP4)

Movie S2 (MP4)

Movie S3 (MP4)

■ AUTHOR INFORMATION

Corresponding Authors

Ali Erdemir – Energy Systems Division, Argonne National Laboratory, Argonne, Illinois 60439, United States; Email: aerdemir@tamu.edu

Jianguo Wen – Center for Nanoscale Materials, Argonne National Laboratory, Argonne, Illinois 60439, United States; orcid.org/0000-0002-3755-0044; Email: jwen@anl.gov

Authors

Giovanni Ramirez – Energy Systems Division, Argonne National Laboratory, Argonne, Illinois 60439, United States; orcid.org/0000-0003-0985-1605

Osman Eryilmaz – Energy Systems Division, Argonne National Laboratory, Argonne, Illinois 60439, United States

Giulio Fatti – Department of Physics, Informatics and Mathematics, University of Modena and Reggio Emilia, 41125 Modena, Italy; orcid.org/0000-0001-7000-7310

Maria Clelia Righi – Department of Physics and Astronomy, University of Bologna, 40127 Bologna, Italy

Complete contact information is available at:

<https://pubs.acs.org/10.1021/acsanm.0c01527>

Notes

The authors declare no competing financial interest.

■ ACKNOWLEDGMENTS

Funding at Argonne National Laboratory was provided by The U.S. Department of Energy, Office of Energy Efficiency and Renewable Energy, Vehicle Technologies and Advanced Manufacturing Offices under Contract DE-AC02-06CH11357. The U.S. Department of Energy, Office of Science User Facility, and supported by the U.S. Department of Energy, Office of Science, under Contract No. DE-AC02-06CH11357.

M.C.R. acknowledges support by the University of Modena and Reggio Emilia through the FAR project and by the European Union through the MAX Centre of Excellence (Grant No. 676598). We thank Dave Gosztola for his support with the Raman measurements at the Center of Nanoscale Materials, Argonne National Laboratory.

■ REFERENCES

- (1) Hsu, S. M.; Zhang, J.; Yin, Z. The Nature and Origin of Tribochemistry. *Tribol. Lett.* **2002**, *13* (2), 131–139.
- (2) Kajdas, C.; Hiratsuka, K. Tribochemistry, Tribocatalysis, and the Negative-Ion-Radical Action Mechanism. *Proc. Inst. Mech. Eng., Part J.* **2009**, *223* (6), 827–848.
- (3) Spikes, H. The History and Mechanisms of ZDDP. *Tribol. Lett.* **2004**, *17* (3), 469–489.
- (4) Erdemir, A.; Eryilmaz, O. Achieving Superlubricity in DLC Films by Controlling Bulk, Surface, and Tribochemistry. *Friction* **2014**, *2* (2), 140–155.
- (5) Donnet, C.; Erdemir, A. Historical Developments and New Trends in Tribological and Solid Lubricant Coatings. *Surf. Coat. Technol.* **2004**, *180–181*, 76–84.
- (6) Sutor, P. Solid Lubricants: Overview and Recent Developments. *MRS Bull.* **1991**, *16* (05), 24–30.

- (7) Bowden, F. P.; Young, J. E. Friction of Diamond, Graphite, and Carbon and the Influence of Surface Films. *Proc. R. Soc. London A: Math. Phys. Eng. Sci.* **1951**, *208* (1095).
- (8) Guo, W.; Yin, J.; Qiu, H.; Guo, Y.; Wu, H.; Xue, M. Friction of Low-Dimensional Nanomaterial Systems. *Friction* **2014**, *2* (3), 209–225.
- (9) Berman, D.; Erdemir, A.; Sumant, A. V. Approaches for Achieving Superlubricity in Two-Dimensional Materials. *ACS Nano* **2018**, *12* (3), 2122–2137.
- (10) Berman, D.; Erdemir, A.; Sumant, A. V. Graphene: A New Emerging Lubricant. *Mater. Today* **2014**, *17* (1), 31–42.
- (11) Zhang, R.; Ning, Z.; Zhang, Y.; Zheng, Q.; Chen, Q.; Xie, H.; Zhang, Q.; Qian, W.; Wei, F. Superlubricity in Centimetres-Long Double-Walled Carbon Nanotubes under Ambient Conditions. *Nat. Nanotechnol.* **2013**, *8* (12), 912–916.
- (12) Erdemir, A.; Donnet, C. Tribology of Diamond-like Carbon Films: Recent Progress and Future Prospects. *J. Phys. D: Appl. Phys.* **2006**, *39* (18), R311–R327.
- (13) Smil, V. Natural Gas: Fuel for the 21st Century.
- (14) Zhang, Y.; Zhang, L.; Zhou, C. Review of Chemical Vapor Deposition of Graphene and Related Applications. *Acc. Chem. Res.* **2013**, *46* (10), 2329–2339.
- (15) Kozlov, S. M.; Viñes, F.; Görling, A. Bonding Mechanisms of Graphene on Metal Surfaces. *J. Phys. Chem. C* **2012**, *116* (13), 7360–7366.
- (16) Kim, K. S.; Zhao, Y.; Jang, H.; Lee, S. Y.; Kim, J. M.; Kim, K. S.; Ahn, J.-H.; Kim, P.; Choi, J.-Y.; Hong, B. H. Large-Scale Pattern Growth of Graphene Films for Stretchable Transparent Electrodes. *Nature* **2009**, *457* (7230), 706–710.
- (17) Reina, A.; Jia, X.; Ho, J.; Nezich, D.; Son, H.; Bulovic, V.; Dresselhaus, M. S.; Kong, J. Large Area, Few-Layer Graphene Films on Arbitrary Substrates by Chemical Vapor Deposition. *Nano Lett.* **2009**, *9* (1), 30–35.
- (18) Patera, L. L.; Africh, C.; Weatherup, R. S.; Blume, R.; Bhardwaj, S.; Castellarin-Cudia, C.; Knop-Gericke, A.; Schloegl, R.; Comelli, G.; Hofmann, S.; Cepek, C. *In Situ* Observations of the Atomistic Mechanisms of Ni Catalyzed Low Temperature Graphene Growth. *ACS Nano* **2013**, *7* (9), 7901–7912.
- (19) Kwon, H.; Choi, S.; Thompson, L. T. Vanadium Nitride Catalysts: Synthesis and Evaluation For n-Butane Dehydrogenation. *J. Catal.* **1999**, *184* (1), 236–246.
- (20) OYAMA, S. Kinetics of Ammonia Decomposition on Vanadium Nitride. *J. Catal.* **1992**, *133* (2), 358–369.
- (21) Ramanathan, S.; Oyama, S. T. New Catalysts for Hydroprocessing: Transition Metal Carbides and Nitrides. *J. Phys. Chem.* **1995**, *99* (44), 16365–16372.
- (22) Franz, R.; Mitterer, C. Vanadium Containing Self-Adaptive Low-Friction Hard Coatings for High-Temperature Applications: A Review. *Surf. Coat. Technol.* **2013**, *228*, 1–13.
- (23) Lim, S. C.; Ashby, M. F. Wear-Mechanism Maps. *Acta Metall.* **1987**, *35* (1), 1–24.
- (24) Mori, S.; Yoshida, M. Decomposition of Aromatic Compounds on Cut Nickel Surface. *Tribol. Trans.* **1988**, *31* (1), 128–132.
- (25) Mori, S. Adsorption of Benzene on the Fresh Steel Surface Formed by Cutting under High Vacuum. *Appl. Surf. Sci.* **1987**, *27* (4), 401–410.
- (26) Lu, R.; Kobayashi, K.; Nanao, H.; Mori, S. Deactivation Effect of Tricresyl Phosphate (TCP) on Tribochemical Decomposition of Hydrocarbon Oil on a Nascent Steel Surface. *Tribol. Lett.* **2009**, *33* (1), 1–8.
- (27) Klinke, D. J.; Wilke, S.; Broadbelt, L. J. A Theoretical Study of Carbon Chemisorption on Ni(111) and Co(0001) Surfaces. *J. Catal.* **1998**, *178* (2), 540–554.
- (28) Burghgraef, H.; Jansen, A. P. J.; van Santen, R. A. Methane Activation and Dehydrogenation on Nickel and Cobalt: A Computational Study. *Surf. Sci.* **1995**, *324* (2–3), 345–356.
- (29) Abild-Pedersen, F.; Lytken, O.; Engbæk, J.; Nielsen, G.; Chorkendorff, I.; Nørskov, J. K. Methane Activation on Ni(1 1 1): Effects of Poisons and Step Defects. *Surf. Sci.* **2005**, *590* (2–3), 127–137.
- (30) Watwe, R. M.; Bengaard, H. S.; Rostrup-Nielsen, J. R.; Dumesic, J. A.; Nørskov, J. K. Theoretical Studies of Stability and Reactivity of CH_x Species on Ni(111). *J. Catal.* **2000**, *189* (1), 16–30.
- (31) Kalin, M. Influence of Flash Temperatures on the Tribological Behaviour in Low-Speed Sliding: A Review. *Mater. Sci. Eng., A* **2004**, *374* (1–2), 390–397.
- (32) Kong, J.; Xiong, D.; Li, J.; Yuan, Q.; Tyagi, R. Effect of Flash Temperature on Tribological Properties of Bulk Metallic Glasses. *Tribol. Lett.* **2009**, *35* (3), 151–158.
- (33) An, W.; Zeng, X. C.; Turner, C. H. First-Principles Study of Methane Dehydrogenation on a Bimetallic Cu/Ni(111) Surface. *J. Chem. Phys.* **2009**, *131* (17), 174702.
- (34) Zilibotti, G.; Corni, S.; Righi, M. C. Load-Induced Confinement Activates Diamond Lubrication by Water. *Phys. Rev. Lett.* **2013**, *111* (14), 146101.
- (35) Kajita, S.; Righi, M. C. A Fundamental Mechanism for Carbon-Film Lubricity Identified by Means of Ab Initio Molecular Dynamics. *Carbon* **2016**, *103*, 193–199.
- (36) Loehlé, S.; Righi, M. Ab Initio Molecular Dynamics Simulation of Tribochemical Reactions Involving Phosphorus Additives at Sliding Iron Interfaces. *Lubricants* **2018**, *6* (2), 31.
- (37) Shibuta, Y.; Arifin, R.; Shimamura, K.; Oguri, T.; Shimojo, F.; Yamaguchi, S. Ab Initio Molecular Dynamics Simulation of Dissociation of Methane on Nickel(1 1 1) Surface: Unravelling Initial Stage of Graphene Growth via a CVD Technique. *Chem. Phys. Lett.* **2013**, *565*, 92–97.
- (38) Liao, Y.; Pourzal, R.; Wimmer, M. A.; Jacobs, J. J.; Fischer, A.; Marks, L. D. Graphitic Tribological Layers in Metal-on-Metal Hip Replacements. *Science* **2011**, *334* (6063), 1687–1690.
- (39) Erdemir, A.; Ramirez, G.; Eryilmaz, O. L.; Narayanan, B.; Liao, Y.; Kamath, G.; Sankaranarayanan, S. K. R. S. Carbon-Based Tribofilms from Lubricating Oils. *Nature* **2016**, *536* (7614), 67–71.
- (40) Fuadi, Z.; Adachi, K.; Muhammad, T. Formation of Carbon-Based Tribofilm Under Palm Methyl Ester. *Tribol. Lett.* **2018**, *66* (3), 88.
- (41) Restuccia, P.; Righi, M. C. Tribochemistry of Graphene on Iron and Its Possible Role in Lubrication of Steel. *Carbon* **2016**, *106*, 118–124.
- (42) Marchetto, D.; Restuccia, P.; Ballestrazzi, A.; Righi, M. C.; Rota, A.; Valeri, S. Surface Passivation by Graphene in the Lubrication of Iron: A Comparison with Bronze. *Carbon* **2017**, *116*, 375–380.
- (43) Oliver, W. C.; Pharr, G. M. An Improved Technique for Determining Hardness and Elastic Modulus Using Load and Displacement Sensing Indentation Experiments. *J. Mater. Res.* **1992**, *7* (6), 1564–1583.
- (44) Perdew, J. P.; Burke, K.; Ernzerhof, M. Generalized Gradient Approximation Made Simple. *Phys. Rev. Lett.* **1996**, *77* (18), 3865–3868.
- (45) Giannozzi, P.; Baroni, S.; Bonini, N.; Calandra, M.; Car, R.; Cavazzoni, C.; Ceresoli, D.; Chiarotti, G. L.; Cococcioni, M.; Dabo, I.; Dal Corso, A.; de Gironcoli, S.; Fabris, S.; Fratesi, G.; Gebauer, R.; Gerstmann, U.; Gougoussis, C.; Kokalj, A.; Lazzeri, M.; Martin-Samos, L.; Marzari, N.; Mauri, F.; Mazzarello, R.; Paolini, S.; Pasquarello, A.; Paulatto, L.; Sbraccia, C.; Scandolo, S.; Sclauzero, G.; Seitsonen, A. P.; Smogunov, A.; Umari, P.; Wentzcovitch, R. M. QUANTUM ESPRESSO: A Modular and Open-Source Software Project for Quantum Simulations of Materials. *J. Phys.: Condens. Matter* **2009**, *21* (39), 395502.